JOURNAL OF PHYSICAL ORGANIC CHEMISTRY, VOL. 4, 135–140 (1991)

REACTIVITY IN RADICAL ABSTRACTION REACTIONS: APPLICATION OF THE CURVE CROSSING MODEL

ADDY PROSS*

Department of Chemistry, Rutgers, The State University of New Jersey New Brunswick, NJ 08903, U.S.A

HIROSHI YAMATAKA

Institute of Scientific and Industrial Research, Osaka University, Ibaraki, Osaka 567, Japan

AND

SHIGERU NAGASE

Department of Chemistry, Yokahama National University, Hodogaya, Yokahama 240, Japan

The curve crossing model was applied to a series of hydrogen abstraction reactions from a family of alkanes, RH (R = methyl, ethyl, isopropyl, tert-butyl) by alkyl, hydrogen and chlorine radicals. The analysis was based on quantitative data obtained from an *ab initio* MO study. Schematic reaction profiles for the reaction of RH with alkyl and hydrogen radicals are built up from just two configurations: reactant, DA, and product $D^{3*}A$. For the Cl atom reaction, however, a significant contribution of D^+A^-, a charge-transfer configuration, is also shown to be present. A simple explanation for differences in the intrinsic barrier for the identity radical abstraction reaction based on the initial gap size between DA and $D^{3*}A$ configurations is provided. The influence of the D^+A^- configuration on the nature of the transition state of the Cl atom reaction and its intrinsic barrier is described. It is the D^+A^- configuration that is responsible for the polar character often observed in radical abstraction and addition reactions.

INTRODUCTION

The factors governing barrier heights in radical abstraction reactions are not yet well understood. To what extent are the barrier heights for simple radical reactions, such as those shown in equations (1)–(3), are governed by thermodynamic considerations and what, if any, are the non-thermodynamic factors that influence reactivity in these systems? Also, it is not known what factors govern the barriers to an identity exchange reaction [equation (3)] where no thermodynamic driving force is present, or what the relationship is between the transition-state (TS) structure and reaction exothermicity in these reactions.

In this paper, we analyse the results of a theoretical study on radical abstraction by $H^{\cdot}$, $Cl^{\cdot}$ and $R^{\cdot}$ from a family of alkanes, R—H [equations (1)–(3)]:

$$R{-}H + {}^{\cdot}H \rightarrow R^{\cdot} + H{-}H \quad (1)$$

$$R{-}H + {}^{\cdot}Cl \rightarrow R^{\cdot} + H{-}Cl \quad (2)$$

$$R{-}H + {}^{\cdot}R \rightarrow R^{\cdot} + H{-}R \quad (3)$$

The study is based on *ab initio* MO calculations on the above systems reported recently,[1,2] and some higher level calculations reported here. The quantitative results are interpreted using the curve crossing model,[3] which provides a qualitative framework for considering the quantitative data. This enables the key factors governing reactivity in these systems to be isolated and better understood.

THEORY

In order to apply the curve crossing model[3] to a radical abstraction reaction, one needs to describe the electronic configuration of the reactants and products for such a process. For any three-electron system two doublet states exist.[4] For H abstraction from R—H by an H atom, these two states may be very simply represented by the two configurations shown in **1** and **2**, respectively. Configuration **1**, termed the reactant configuration, shows the three-group–three-electron system in an electronic configuration that couples up

$R^{\uparrow}\ {}^{\downarrow}H\ {}^{\downarrow}H$ — DA — **1**

$R^{\uparrow}\ {}^{\uparrow}H\ {}^{\downarrow}H$ — $D^{3*}A$ — **2**

*On sabbatical leave at Rutgers University, 1989–90. Permanent address: Department of Chemistry, Ben-Gurion University of the Negev, Beer-Sheva 84105, Israel.

0894–3230/91/030135–06$05.00

Received 4 June 1990
Revised 25 September 1990

the two odd electrons on R and H to form the R—H bond. In contrast, the two odd electrons on the two H atoms are uncoupled, so that this configuration precludes H—H bond formation.[5] Hence the reactant configuration provides a proper description of the reactants and may be designated DA (where R—H is the donor, D, and H the acceptor, A). In the product configuration, **2**, however, it is the two odd electrons in the R—H bond that are now uncoupled, while the two odd electrons on the H atoms are coupled together in a singlet pair. Hence this electronic configuration provides an electronic description of the reaction products, R˙ and H—H. Since the two electrons in the R—H portion in **2** are uncoupled, the R—H linkage is a locally excited one with respect to the singlet electron pair. This local excitation is best approximated by a triplet pair (as implied by the representation of **2**) and may therefore be denoted by the designation $D^{3*}A$. (The actual excited state that describes the products does not strictly incorporate the R—H bond in its triplet state. The triplet state is merely a state that usefully represents the fact that the R—H electron pair in **2** is not a bonding pair. The actual initial energy gap between reactant, **1**, and product **2**, configurations is not equal to ΔE_{ST}, the singlet–triplet energy gap, but may be shown to be *ca* $0{\cdot}75\Delta E_{ST}$. For a detailed analysis, see Ref. 5a, b.)

An energy plot of reactant (DA) and product ($D^{3*}A$) configurations as a function of the reaction coordinate is illustrated in Figure 1. Initially, at the reactant geometry, the reactant configuration is low in energy. However, as the central H atom is transferred from R to the H radical (the reaction coordinate) the energy rises; the R—H bond is stretched while it is replaced by a triplet destabilizing H—H interaction. The product configuration, ($D^{3*}A$), does the reverse. In the reactant

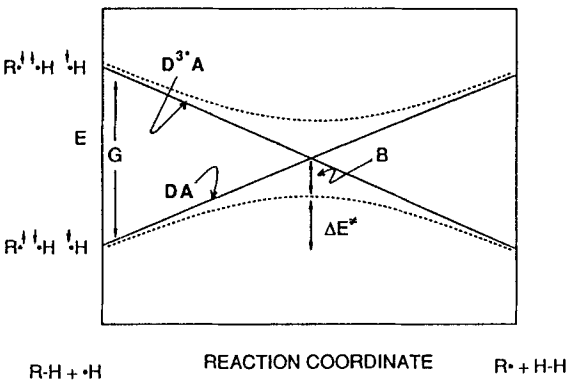

Figure 1. Schematic energy diagram for the avoided crossing of reactant, **1**, (DA) and product, **2**, ($D^{3*}A$) configurations for the reaction R—H + ·H → R· + H—H. Dashed curves represent the resultant reaction surfaces (ground and excited) after configuration mixing

geometry it is high in energy since now the R—H interaction is that between electrons of the same spin, i.e. a triplet interaction. In this geometry the stabilizing H—H singlet (i.e. bonding) interaction is absent owing to the large H—H distance. However, as the system moves along the reaction coordinate, its energy drops; the R—H destabilizing triplet interaction is removed while the stabilizing H—H singlet interaction (i.e. bond formation) is brought about. Let us consider the relationship between the reactant and product configurations. It is clear that in the reactant geometry the product configuration, ($D^{3*}A$), represents an excited electronic configuration with respect to DA; in order to generate $D^{3*}A$ from DA, the R—H bond needs to be excited from the singlet to the triplet state (D to D^{3*}) (see comments above regarding the actual excited state).

The actual ground energy surface for the H atom abstraction reaction is represented by the lower dashed curve in Figure 1. The dashed curves come about as a result of the avoided crossing of the two configuration curves, DA and $D^{3*}A$. Hence the barrier to the reaction may be formulated as[3]

$$\Delta E^{\neq} = fG - B \tag{4}$$

where $\Delta E^{\neq}$ is the reaction barrier, G is the initial energy gap between **1** and **2**, in this case related to the singlet–triplet energy gap for the R—H bond, f is a fraction in the range 0–1 and B is the avoided crossing quantum mechanical mixing term.[3] Since the TS for this reaction lies in that part of the reaction coordinate where the reactant and product configurations are of similar energy, the electronic description of the TS may be described by a resonance hybrid of DA and $D^{3*}A$:

$$TS = R^{\uparrow}\ {}^{\downarrow}H\ {}^{\downarrow}H \quad \leftrightarrow \quad R^{\uparrow}\ {}^{\uparrow}H\ {}^{\downarrow}H \tag{5}$$

For H abstraction from R—H by a Cl atom [equation (2)], a two-configuration description for building up the reaction surface is not adequate. Hence, for this reaction, in addition to reactant and product configurations, DA, **3**, and $D^{3*}A$, **4**, a third (intermediate) configuration, involving charge transfer between R—H and Cl ($D^{+}A^{-}$), **5**, becomes important.

$R^{\uparrow}\ {}^{\downarrow}H\ {}^{\downarrow}Cl$	$R^{\uparrow}\ {}^{\uparrow}H\ {}^{\downarrow}Cl$	$(R-H)^{+\cdot}\ :Cl^{-}$
DA	$D^{3*}A$	$D^{+}A^{-}$
3	**4**	**5**

This is because the Cl atom is a better acceptor ($EA = 83$ kcal mol^{-1})[6] than the H atom ($EA = 19$ kcal mol^{-1}),[6,7] (1 kcal = 4·2 kJ) so that the energy of the $D^{+}A^{-}$ configuration is relatively low and may be similar to that of $D^{3*}A$. As a result, it may contribute significantly to a description of the reaction profile. An energy diagram showing the formation of the ground reaction surface for the Cl atom abstraction reaction is shown in Figure 2. The three contributing configuration curves, DA, $D^{3*}A$, and $D^{+}A^{-}$ are represented, in addition to the resultant energy surface

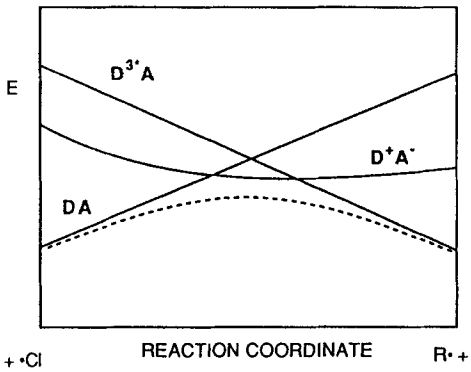

Figure 2. Schematic energy diagram showing reactant, **3**, (DA), product, **4**), ($D^{3*}A$) and intermediate, **5**, ($D^{+}A^{-}$) configurations for the reaction R—H + Cl → R· + H—Cl. Dashed curve represents the ground-state surface that results from the mixing of these three configurations

(dashed line). Since in the TS region all three configurations contribute to the electronic structure, the TS for the Cl atom abstraction reaction may be described as a resonance hybrid of all three configurations, as indicated in the equation

$$TS = R^{\uparrow}\cdot\ {}^{\downarrow}H\ {}^{\downarrow}Cl \quad \leftrightarrow \quad R^{\uparrow}\ {}^{\uparrow}H\ \cdot Cl \quad \leftrightarrow \quad (R-H)^{+\cdot}\ :Cl^{-} \quad (6)$$

On the basis of the foregoing qualitative description, we now discuss the computational data for the three reactions, equations (1)–(3).

COMPUTATIONAL METHOD AND RESULTS

Results of the *ab initio* MO calculations for the reactions in equations (1)–(3) (R = methyl, ethyl, isopropyl, *tert*-butyl) at the MP2/6–31G*//UHF/3–21G level were previously reported in Ref. 1 and are shown in Tables 1–3. In view of unexpected differences in the TS structural data for the H abstraction and Cl abstraction reactions, the data for reactions (1) and (2) were reoptimized at the 6–31G* level using the Gaussian 88 program.[8] This enables us to establish whether the difference in the TS structures for the two systems is a real one or merely a computational artefact. Data for reactions (1) and (2) at the higher MP2/6–31G*//UHF/6–31G* level are listed in Tables 2 and 3.

Table 1. Calculated barriers for identity reactions: R—H + ·R → R· + H—R [equation (3)] [a]

R	Barrier height (kcal mol^{-1})
Me	22·4 (25·2)[b]
Et	20·5
i-Pr	18·2
t-Bu	15·3

[a] Data taken from Ref. 1 and calculated at the MP2/6–31G*//3–21G level.
[b] Calculated at the MP3/6–31G**//6–31G** level.[1]

Table 2. Calculated transition-state C—H bond lengths, activation energies, $\Delta E^{\neq}$, reaction energies, ΔE, and intrinsic barriers $\Delta E_0^{\neq}$, for R—H + ·H → R· + H—H [equation (1)] [a]

Parameter	Me—H—H	Et—H—H	*i*-Pr—H—H	*t*-Bu—H—H
r_{C-H}[b]	1·377	1·362	1·348	1·355
r_{H-H}[b]	0·924	0·939	0·951	0·964
n_{C-H}[c]	0·377	0·399	0·419	0·444
n_{H-H}[c]	0·524	0·498	0·478	0·458
$\Delta E^{\neq}$[d]	25·6	22·9	20·4	18·2
ΔE[d]	11·2	8·3	5·8	3·8
$\Delta E_0^{\neq}$[d,e]	19·6	18·5	17·4	16·2

[a] Calculated at the MP2/6–31G*//6–31G* level
[b] Bond lengths in ångstroms.
[c] Pauling bond order calculated with equation (9) in Ref. 1.
[d] In kcal mol^{-1}.
[e] Calculated using the form of Marcus equation [(equation (11), Ref. 1]), which should read

$$\Delta E_0^{\neq} = \tfrac{1}{2}\{\Delta E^{\neq} - \tfrac{1}{2}\Delta E + [\Delta E^{\neq}(\Delta E^{\neq} - \Delta E)]^{1/2}\}.$$

Table 3. Calculated transition-state C—H bond lengths, activation energies, $\Delta E^{\neq}$, reaction energies, ΔE, and intrinsic barriers $\Delta E_0^{\neq}$, for R—H + ·Cl → R· + H—Cl [equation (1)] [a]

Parameter	Me—H—Cl	Et—H—Cl	*i*-Pr—H—Cl	*t*-Bu—H—Cl
r_{C-H}[b]	1·397	1·381	1·365	1·348
r_{H-Cl}[b]	1·475	1·489	1·505	1·522
n_{C-H}[c]	0·352	0·374	0·396	0·422
n_{H-Cl}[c]	0·500	0·477	0·452	0·427
$\Delta E^{\neq}$[d]	18·0	12·7	8·0	4·2
ΔE[d]	12·8	9·1	5·9	3·3
$\Delta E_0^{\neq}$[d,e]	10·6	7·5	4·6	2·2

[a] Calculated at the MP2/6–31G*//6–31G* level
[b] Bond lengths in ångstroms.
[c] Pauling bond order calculated with equation (9) in Ref. 1.
[d] In kcal mol^{-1}.
[e] Calculated using the form of Marcus equation [(equation (11), Ref. 1]), which should read

$$\Delta E_0^{\neq} = \tfrac{1}{2}\{\Delta E^{\neq} - \tfrac{1}{2}\Delta E + [\Delta E^{\neq}(\Delta E^{\neq} - \Delta E)]^{1/2}\}.$$

DISCUSSION

Barrier heights in identity exchange reaction

Let us first consider the effects of different alkyl groups, R, on the barrier for the identity H atom transfer reaction [equation (3)]. It is not clear, *a priori*, whether the barrier resulting from electronic factors will

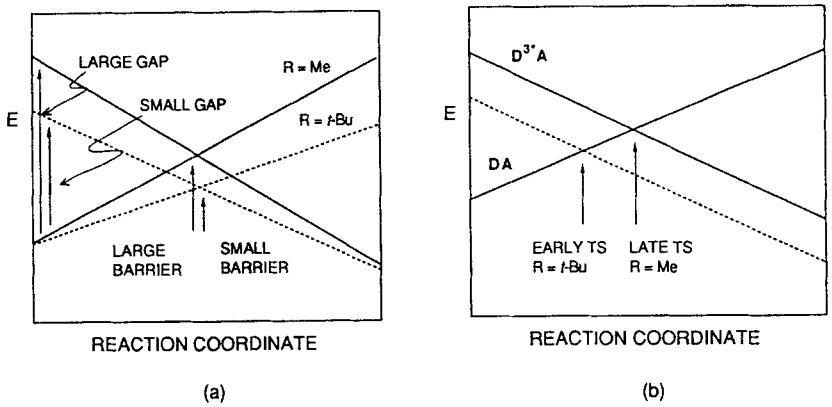

Figure 3. (a) Schematic energy diagram showing the effect of initial energy gap size on barrier height for the identity reaction R—H + ·R → R· + H—R. A large gap size (strong R—H bond as in Me—H), indicated by solid lines, leads to a large reaction barrier, while a small gap size (weak R—H bond as in *t*-Bu—H), indicated by dashed lines, leads to a small reaction barrier. (b) Schematic energy diagram showing the effect of stabilization of the product configuration, $D^{3*}A$, on the position of the TS along the reaction coordinate. Stabilization of $D^{3*}A$, [e.g. obtained by replacing R = Me by *t*-Bu in equation (1)] leads to an earlier TS. Dashed line represents stabilized *t*-Bu configuration

increase, decrease or remain constant, as a function of different alkyl groups. Knowing the relative R—H bond strengths does not, in itself, provide an answer. For example, breaking the stronger Me—H bond in the TS will have the effect of raising the TS energy, compared with breaking the weaker *t*-Bu—H bond. However, concurrent formation of a stronger Me—H bond will also have the effect of stabilizing the TS. Since for such a process the TS is symmetrical, which effect will dominate, bond breaking or bond making? Since there is no thermodynamic driving force for this series of identity processes, current models for considering reactivity, such as the Marcus theory[9] and potential energy surface diagrams,[10] fail to predict the reactivity trend in such a reaction family.

The curve crossing model[3] provides a simple answer to this question. The energy diagram for this reaction [equation (3)], for R = Me and R = *t*-Bu, is illustrated in Figure 3(a). As discussed above, the reaction surface for a radical abstraction reaction may be described by the avoided crossing of DA and $D^{3*}A$ configurations. For R = Me the initial DA–$D^{3*}A$ energy gap is large since the Me—H bond strength is large (104 kcal mol^{-1}).[11] This is because the R—H singlet–triplet energy gap is directly related to the R—H bond strength,[5b] which decreases in the order Me—H > Et—H > *i*-Pr—H > *t*-Bu—H.[11] The barrier for this process is thus approximated by the crossing point of the bold lines. For R = *t*-Bu, however, the gap is smaller (the *t*-Bu—H bond strength is just 91 kcal mol^{-1}),[11] so that barrier formation may be represented by the crossing point of the dashed lines. While the above analysis ignores the effect of variation in the *f* factor, this is assumed to be slight for a family of different alkyl radicals, at least in comparison with the widely varying *G* values.

Consequently, by simple application of the curve crossing model, one can predict that the barrier to the radical identity exchange reaction will be related to the R—H bond strength: the greater the bond strength, the larger is the barrier. This behaviour is confirmed computationally (Table 1). The intrinsic barrier for the identity exchange reaction [equation (3)] decreases in the order Me—H > Et—H > *i*-Pr—H > *t*-Bu—H, as predicted. Although the computed values do not accurately represent the experimental barrier, we believe the trend manifested in the data in Table 1 to be significant. (The experimental Arrhenius activation barrier for $CH_3—H + CH_3 \rightarrow CH_3 + H—CH_3$ has been reported as being *ca* 14·7 kcal mol^{-1}.[12] This is significantly less than the computed values reported here and elsewhere;[13] however, it has been pointed out recently[13] that the true adiabatic barrier is not directly comparable with the experimental Arrhenius activation barrier and must exceed 18·4 kcal mol^{-1}). The effect of gap size on reactivity, using the curve crossing models, has been discussed previously for a variety of organic reactions.[3]

Abstraction by H atom

TS structure

Examination of the data in Table 2 reveals that the structure of the TS in the reaction of R—H with H· changes in a regular way as a function of the reaction energy. The more endothermic the reaction, the later is the TS in geometric terms. Thus, for example, the

relatively endothermic reaction of Me—H with $H^{\cdot}$ ($\Delta E = 11{\cdot}2$ kcal mol^{-1}) has a C—H bond that is more stretched in the TS ($n_{C-H} = 0{\cdot}377$) than for the less endothermic reaction of *t*-Bu—H with $H^{\cdot}$ ($\Delta E = 3{\cdot}8$ kcal mol^{-1}, $n_{C-H} = 0{\cdot}444$). This is in accord with the Leffler–Hammond postulate,[14,15] which suggests that TS geometry and reaction exothermicity are related.

Consideration of the curve crossing diagram for this reaction leads to conclusions that are consistent with the Leffler–Hammond postulate. For this system, the curve crossing diagram is analogous to a Bell–Evans–Polanyi diagram (Figure 3b).[16] On changing the substrate from Me—H to Et—H to *i*-Pr—H to *t*-Bu—H, the $D^{3*}A$ energy curve is stabilized at both reaction ends. It is stabilized at the reactant end because the singlet-triplet energy gap, *G* (related to the difference in energy between reactant and product configurations at the reactant geometry, see Figure 1), becomes smaller as the R—H bond weakens (discussed above for the identity reaction). It is also stabilized at the product end because breaking the weaker C—H bond leads to a less endothermic reaction. The effect of stabilizing the $D^{3*}A$ configuration is shown in Figure (3b). As $D^{3*}A$ is stabilized (dashed line), the barrier (as approximated by the crossing point) is lowered and the TS becomes earlier along the reaction coordinate, consistent with the Leffler–Hammond postulate and the computational data (Table 2).

It is commonly believed that a plot of activation barriers ($\Delta E^{\neq}$) versus the heat of reaction (ΔE) for a particular reaction family provides a measure of TS structure. However, as has been pointed out earlier,[1,17] there is no simple relationship between the slope, α, of the $\Delta E^{\neq}$ versus ΔE plot ($\alpha = 1{\cdot}0$) and the position of the TS along the reaction coordinate for the H atom abstraction reaction. Despite the large value of α, supposedly indicative of a product-like TS, the computed structure of the TS is actually one in which the H atom is about half transferred (Table 2). We reaffirm the danger in using rate–equilibrium correlations as quantitative measures of TS structure.[17]

Intrinsic barriers

Intrinsic barriers, $\Delta E_0^{\neq}$, for the family of reactions with H atom [equation (1)], calculated by substituting $\Delta E^{\neq}$ and ΔE° values into the Marcus equation, are listed in Table 2. (For the appropriate form of the Marcus equation, see Ref. 1 equation (11), which should read:

$$\Delta E_0^{\neq} = \tfrac{1}{2}\{\Delta E^{\neq} - \tfrac{1}{2}\Delta E + [\Delta E^{\neq}(\Delta E^{\neq} - \Delta E)]_{1/2}\}.)$$

It can be seen that the intrinsic barrier decreases in the order Me—H > Et—H > *i*-Pr—H > *t*-Bu—H. Given the reduction in the identity exchange reaction [equation (3)], discussed above, which follows the same order, and which contributes to the intrinsic barrier of the non-identity reaction, this trend is to be expected.

Abstraction by Cl atom

TS structure

At the MP2/6–31G*//UHF/3–21G level, the Cl atom reaction [equation (2)] differs from the H atom abstraction reaction [equation (1)] in that the structure of the TS is essentially invariant as a function of the reacting alkane, R—H (Table 1, Ref. 1). However, at the higher MP2/6–31G*//UHF/6–31G* level (Table 3), both reactions show the same qualitative behaviour: the less endothermic the reaction, the earlier is the TS. In other words, here also the TS appears to conform to Leffler–Hammond-type behaviour. However, the Cl family does differ from the H atom family in several other respects.

Intrinsic barriers

Calculated intrinsic barriers, $\Delta E_0^{\neq}$, for the Cl reaction [equation (2)] are listed in Table 3. (For the appropriate form of the Marcus equation, see Ref. 1, equation (11), which should read: $\Delta E_0^{\neq} = \tfrac{1}{2}\{\Delta E^{\neq} - \tfrac{1}{2}\Delta E + [\Delta E^{\neq}(\Delta E^{\neq} - \Delta E)]_{1/2}\}$.) It can be seen that there is a much greater reduction in the intrinsic barrier for the Cl family (from 10·6 kcal mol^{-1} for Me—H down to 2·2 kcal mol^{-1} for *t*-Bu—H) compared with the corresponding reduction for the H family (from 19·6 kcal mol^{-1} for Me—H down to 16·2 kcal mol^{-1} for *t*-Bu—H), although both families follow the same order. We have already commented on the reduction in intrinsic barrier for the H family and we now wish to comment on the dramatic drop in the intrinsic barrier for the Cl family.

Since the intrinsic barrier is the barrier in the absence of any thermodynamic driving force, its magnitude is particularly sensitive to the presence of an intermediate configuration. This is because by its very nature the intermediate configuration mixes in strongly in the TS region but only slightly at reactant and product ends of the surface. Thus substituent changes that affect the energy of the intermediate configuration will contribute to changes in the magnitude of the intrinsic barrier, in addition to any effects on the energy of the product configuration, $D^{3*}A$. For the reaction of equation (2), we have pointed out that the charge-transfer configuration, $D^{+}A^{-}$, plays a significant role in describing the TS. Thus in this system, variation in the R group affects the intrinsic barrier not only through the energy gap, *G*, between the reactant and product configurations, (as discussed for the abstraction by an H atom) but also by the extent of $D^{+}A^{-}$ mixing. Thus, when the R group is changed from Me to *t*-Bu, not only is $D^{3*}A$ stabilized, but also the intermediate configuration, $D^{+}A^{-}$ is stabilized, since

t-Bu—H is a better electron donor than Me—H ($IP_{Me-H} = 13{\cdot}0$ eV; $IP_{t\text{-}Bu-H} = 10{\cdot}6$ eV).[18] This is indeed confirmed by the fact that there is more charge transfer from *t*-Bu—H to Cl (−0·22) in the *t*-Bu····H····Cl TS than from Me—H to Cl in the Me····H····Cl TS (−0·19). Consequently, a larger variation in the intrinsic barrier is expected for the reaction with a Cl atom than with an H atom, as observed (Table 3). We see, therefore, that substituent effects on the rates of reaction families described by three configurations are likely to be more dramatic than those described by just two configurations.

A number of characteristics of the Cl atom reaction as observed in the computations now also become clearer. For this reaction family there is substantial charge development in the TS. For example, reactions of methane with Cl and H lead to TS population analyses:

$$\underset{+0{\cdot}14\ \ +0{\cdot}05\ \ -0{\cdot}19}{Me\cdots H\cdots Cl} \qquad \underset{-0{\cdot}04\ \ +0{\cdot}04\ \ 0{\cdot}00}{Me\cdots H\cdots H}$$

The substantial amount of charge transfer from methane to Cl compared with the zero charge transfer from methane to H indeed reflects the contribution of D^+A^- to a description of the reaction surface for the Cl reaction. In fact, the formation of a charge-transfer complex is just another manifestation of the charge-transfer configuration, D^+A^-. The formation of a complex, R····H—Cl, close in energy and structure to the reaction products, R˙ and H—Cl, comes about through the mixing of D^+A^- with the product configuration, $D^{3*}A$. The complex is formed on the product side rather than the reactant side of the reaction because the reaction is endothermic; this means that $D^{3*}A$–D^+A^- mixing at the product end will be larger than DA–D^+A^- mixing at the reactant end since the $D^{3*}A$–D^+A^- energy separation is smaller at the product geometry (greater mixing) than DA–D^+A^- energy separation at the reactant geometry (reduced mixing) (the degree of mixing is inversely proportional to the energy separation).[3c,d] Hence complex formation is more likely to be observed on the high-energy side of the reaction, as is indeed observed.

An additional consequence of the mixing in of a third or 'foreign' configuration is the formation of a flatter reaction surface. Indeed, the flatness of the reaction surface can be gauged by inspecting the magnitude of the force constant for the normal coordinate with the imaginary frequency. For the TS obtained from Cl attack the value is $-2{\cdot}23$ mdyn Å^{-1}, whereas for the TS obtained from H attack the corresponding value is $-3{\cdot}20$ mdyn Å^{-1}. In other words, the reaction surface for attack by Cl is flatter than that for attack by H, as might be expected from the model.

In conclusion, the curve crossing model provides a convenient framework for considering simple radical abstraction reactions. Three main criteria are responsible for governing barrier heights in these systems: (a) the heat of reaction, (b) the singlet–triplet energy gap for the bond being broken (often related to the bond strength) and (c) in those cases where the reactants constitute a good donor–acceptor pair (characterized by a low D^+A^- energy gap), the actual electron-transfer energy from one reactant to the other. It is the contribution of the D^+A^- configuration to the transition states of these systems that leads to the polar character observed in many radical reactions.

REFERENCES

1. H. Yamataka and S. Nagase, *J. Org. Chem.* **53**, 3232 (1988).
2. For a theoretical treatment of radical abstraction and addition reactions, see S. Nagase, K. Takatsuka and T. Fueno, *J. Am. Chem. Soc.* **98**, 3838 (1976). For a recent paper on radical regioselectivity, see S. S. Shaik and E. Canadell, *J. Am. Chem. Soc.* **112**, 1446 (1990).
3. For reviews on the curve crossing (CM and SCD) models, see (a) T. H. Lowry and K. S. Richardson, *Mechanism and Theory in Organic Chemistry*, 3rd Edn, pp. 218–222, 354–360. Harper and Row, New York (1987); (b) A. Pross and S. S. Shaik, *Acc. Chem. Res.* **16**, 363 (1983); (c) S. S. Shaik *Prog. Phys. Org. Chem.* **15**, 197 (1985); (d) A. Pross *Adv. Phys. Org. Chem.* **21**, 99 (1985)
4. See, for example, L. Salem, *Electrons in Chemical Reactions: First Principles*. Wiley, New York, *(1982)*
5. (a) S. S. Shaik and P. C. Hiberty, *J. Am. Chem. Soc.* **107**, 3089 (1985); (b) S. S. Shaik, P. C. Hiberty, J.-M. Lefour and G. Ohanessian, *J. Am. Chem. Soc.* **109**, 363 (1987); (c) S. S. Shaik and R. Bar, *Nouv. J. Chim.* **8**, 411 (1984)
6. K. Tanaka, G. I. Mackay, J. D. Payzant and D. K. Bohme, *Can. J. Chem.* **54**, 1643 (1976)
7. E. C. M. Chen and W. E. Wentworth , *J. Chem Educ.* **52**, 486 (1975).
8. M. J. Frisch, M. Head-Gordon, H. B. Schlegel, K. Raghavachari, J. S. Binkley, C. Gonzales, D. J. DeFrees, D. J. Fox, R. A. Whiteside, R. Seeger, C. F. Melius, J. Baker, R. Martin, L. R. Kahn, J. J. P. Stewart, E. M. Fluder, S. Topiol and J. A. Pople, *Gaussian 88, Release C.* Gaussian, Pittsburgh.
9. (a) R. A. Marcus, *J. Phys. Chem.* **72**, 891 (1968); (b) R. A. Marcus, *Annu. Rev. Phys. Chem.* **15**, 155 (1964).
10. (a) E. R. Thornton, *J. Am. Chem. Soc.* **89**, 2915 (1967); (b) R. A. More O'Ferrall, *J. Chem. Soc. B* 274 (1970); (c) W. P. Jencks, *Chem. Rev.* **72**, 705 (1972).
11. A. J. Gordon and R. A. Ford, *The Chemists Companion* Wiley, New York (1972)
12. F. S. Dainton, K. J. Ivin and F. Wilkinson, *Trans. Faraday Soc.* **55**, 929 (1959); G. A. Creak, F. S. Dainton and K. J. Ivin, *Trans. Faraday Soc.* **58**, 326 (1962).
13. T. A. Wildman, *Chem. Phys. Lett.* **126**, 325 (1986)
14. (a) J. E. Leffler and E. Grunwald, *Rates and Equilibria of Organic Reactions* pp. 128–170. Wiley, New York (1963); (b) J. E. Leffler, *Science* **117**, 340 (1953)
15. G. Hammond, *J. Am. Chem. Soc.* **77**, 334 (1955).
16. (a) R. P. Bell, *Proc. R. Soc. London, Ser. A* **154**, 414 (1936); (b) M. G. Evans and M. Polanyi, *Trans. Faraday Soc.* **32**, 1340 (1936).
17. For a general discussion on the misuse of the Brønsted parameter, see A. Pross and S. S. Shaik, *Nouv. J. Chim.* **13**, 427 (1989).
18. D. W. Turner, *Adv. Phys. Org. Chem.* **4**, 30 (1966).